# Oxide copper nanoparticles stabilized by acrylonitrile and methyl methacrylate polar monomers through a ligand exchange reaction

To cite this article: Bárbara Rodríguez *et al* 2021 *Mater. Res. Express* **8** 045002

Materials Research Express

PAPER

# Oxide copper nanoparticles stabilized by acrylonitrile and methyl methacrylate polar monomers through a ligand exchange reaction

**Bárbara Rodríguez**[1], **Sara Ramírez**[2], **Pablo Gutiérrez**[3], **Nataly Silva**[4], **Isaac Díaz-Aburto**[5], **Andreina García**[1,6] **and Iván Martínez**[3]

[1] Advanced Mining Technology Center (AMTC), Universidad de Chile, Av. Tupper 2007, 8370451 Santiago, Chile
[2] Department of Materials Chemistry, Faculty of Chemistry and Biology, Universidad de Santiago de Chile, Av. Libertador Bernardo O'Higgins 3363, Estación Central, Santiago 9170124, Chile
[3] Departamento de Ciencias Químicas y Biológicas, Universidad Bernardo O´Higgins, General Gana 1702, Santiago, Chile
[4] Facultad de Diseño, Universidad del Desarrollo, Avenida Plaza 680, 7610658 Las Condes, Santiago, Chile
[5] Departamento de Química, Escuela de Química, Facultad de Ciencias Naturales, Matemática y del Medio Ambiente, Universidad Tecnológica Metropolitana, Las Palmeras # 3360, Ñuñoa. Santiago—Chile
[6] Mining Engineering Department, FCFM, Universidad de Chile, Santiago 8370451, Chile

**E-mail:** nrsilva@udd.cl **and** ivan.martinez@ubo.cl

**Keywords:** copper nanoparticle, functionalization, ligand exchange, acrylonitrile, methyl methacrylate

OPEN ACCESS

RECEIVED
25 January 2021

REVISED
11 March 2021

ACCEPTED FOR PUBLICATION
22 March 2021

PUBLISHED
2 April 2021



## Abstract

This research reports the synthesis of copper oxide nanoparticles (CuONP) functionalized by the polar monomers acrylonitrile (ACN) and methyl methacrylate (MMA). The synthesis was achieved by a practical exchange ligand reaction from CuONP previously stabilized by hexadecyltrimethylammonium bromide (CTAB). The replacement of CTAB by ACN or MMA produced the functionalized nanoparticles CuONP-ACN and CuONP-MMA, respectively. The functionalized nanoparticles were characterized by ultraviolet-visible spectroscopy (UV–vis), Fourier transform infrared spectroscopy (FTIR), field emission scanning electron microscopy (SEM), dynamic light scattering (DLS), Zeta potential, x-ray diffraction (XRD), high-resolution-transmission electron microscopy (HR-TEM), and selected area electron diffraction (SAED) analysis. Changes in surface plasmon resonance (SPR) band and the functional group bands observed in UV–vis and FTIR spectra confirmed the efficient replacement of CTAB by polar monomers. Moreover, CuONP-ACN and CuONP-MMA showed a negative surface charge with spherical morphology. X-ray diffraction (XRD) analysis showed that a monoclinic CuO crystal system was formed.

## 1. Introduction

Nanotechnology is an area that has grown rapidly over the last few years and it plays a key role in several emerging technologies [1]. Among the different nanomaterials developed until date, it is possible to find the development of metal nanoparticles (MNP) which exhibit properties remarkably differ from those of the bulk counter part because of quantum size confinement imposed by the nano-size regime. These exceptional properties have allowed their application in several fields. For example, the gold, silver and copper nanoparticles have been applied to sensing, catalysis, and even antimicrobials [2–9]. Particularly, copper nanoparticles metal and oxides (CuNP, CuO and $Cu_2ONP$) have been attractive due to the copper is an element has high natural abundance and low cost. Moreover, there are multiple cost-effective synthesis routes for obtaining copper nanoparticles [10]. In addition, these nanoparticles have excellent antimicrobial activity and their effectiveness to inhibit the growth of pathogenic microorganisms make them ideal candidates to be active biocide agents. In fact, one of the main applications of copper oxide nanoparticles relies on their action as antibiotic, antimicrobial, and antifungal agents when they are added to plastics, coatings, and textiles. When the CuONP are incorporated into different materials, it is necessary to achieve good antibacterial properties without affecting the desired mechanical, optical, electrical, and thermal properties of those materials. In this context, the interfacial interactions between the surface of the CuONP and the polymer matrix play an important role. The NP have a

high specific surface which promotes the formation of aggregates and avoids the achievement of a nanocomposite with well-dispersed nanostructures. This problem could be addressed by changing the surface chemistry of the nanostructures. The properties of copper nanostructures depend on their surface physicochemical features, which are controlled by a synthesis or stabilization process. Several synthesis processes that prepare CuNP and CuONP with tunable compositions, shapes, sizes, and structures have been reported. Chemical, physical, and biological methods have been employed to synthesize CuNP and CuONP [11]. Among the chemical methods used to obtain CuNP and CuONP are the photochemical method, electrochemical method, thermal decomposition method, and chemical reduction method, with the last method being the one that is most frequently used to obtain stable, colloidal dispersions in aqueous and organic solvents [12]. The chemical reduction method implies the use of a source of copper ions, a reducing agent, and stabilizing or capping agent. The source of the copper ions most used to synthesize CuONP is copper salts such as sulfate, chloride, and acetate [13] These copper ions are reduced by reducing agents to produce nucleus/cluster metal nascent that subsequently nucleates and grows to generate the final nanoparticle, as this nanoparticle increases, the reducing strength increases the speed of nucleation. The reducing agents employed including sodium borohydride [13], ascorbic acid [14], hydrazine [15], sodium citrate [16], among others [17]. The stabilizing agents, also known as capping agents, have the main functions of preventing the uncontrollable growth of particles, preventing particle aggregation, controlling the growth rate, controlling particle size, and allowing for particle solubility in several solvents. These functions have been achieved by steric stabilization employing sterically bulky polymers (polyvinyl alcohol (PVA) [16, 18, 19], polyethylene glycol (PEG), and polypropylene glycol (PPG) [16, 18, 19], polyethylene glycol (PEG), and polypropylene glycol (PPG) [17]), and by electrostatic stabilization employing surfactants (Hexadecyltrimethylammonium bromide (CTAB) [19–21], hexamethylene tetramine (HTMA) [22], and tetramethylammonium hydroxide (TMAH) [23]). It has been observed that properties such as the morphology and size of CuONP can be controlled by the molar ratio of copper ions: reducing agents: stabilizer agents [13].

Additionally, another strategy for modifying the surfaces of the metal and metal oxide nanostructures is exchanging the existing capping agents for others. The functionalization of heavy-metal chalcogenide nanocrystal (CdSe, PbS) by the exchange ligand process has been widely studied [24]. On the other hand, several studies have reported the functionalization of AuNP surface with different ligands by a ligand exchange reaction. The ligands principally used including different types of thiolated molecules [25], 11-mercaptoundecanoic acid [26], oleylamine, octadecanethiol [27], polyethylene glycol and polyvinylpyrrolidone [28]. Iron oxide magnetic nanoparticles have also been functionalized by the exchange ligand process and the ligands used including cysteine, 5-aminovaleric acid, glutathione [29], citric acids [30] , polyethylene glycol with different functional group [31], 4-hydroxi benzoic acid, 3-(4-hydroxyphenyl)propionic acid, gallic acid [30], ricinoleic acid, galataric acid, 2-bromo-2-methyl propionic acid, and succinic anhydride [30].

Despite several studies involving the functionalization of nanoparticles by exchange ligand with organic molecules with different functional groups, to the best of our knowledge, there is no precedent in the literature regarding the functionalization of CuONP by the exchange ligand process.

Recently, our group reported a method for the simple, quick, and reproducible synthesis of CuONP from a metal copper cluster [31]. In this synthesis, the capping agent used was CTAB. We have envisaged exploring the surface modification of this new CuONP by exchange ligand reaction. Among the principal polar monomers used in the polymer industry are acrylonitrile (ACN) and methyl methacrylate (MMA), which contain the functional group nitrile and esther, respectively. In this context, we herein report the synthesis and characterization of two new copper oxide nanoparticles, CuONP-ACN and CuONP-MMA, functionalized with ACN and MMA neutral ligands by the exchange ligand reaction. Furthermore, we found that the CTAB replacement by polar monomers affected the Zeta potential, size, and surface plasmon resonance (SPR) band of synthesized nanoparticles.

## 2. Methodology

### 2.1. Materials

All chemicals of analytical grade—copper (II) sulfate pentahydrate salt ($CuSO_4{\cdot}5H_2O$) (98%) and sodium hydroxide (NaOH) (≈99%)—were obtained from Merck. Cetyltrimethylammonium bromide (CTAB) (>99%), sodium borohydride ($NaBH_4$) (99.99%), acrylonitrile ($C_3H_3N$) (>99%), and methyl acrylate ($C_4H_6O_2$) (99%) were procured from Sigma. The CuONP stabilized by CTAB were produced by ultrasound-assisted chemical reduction (digital ultrasonic BIOBASE, model UC-20A, 40 KHz). The CuONP stabilized by polar monomers were produced by ligand exchange reaction used magnetic stirring.

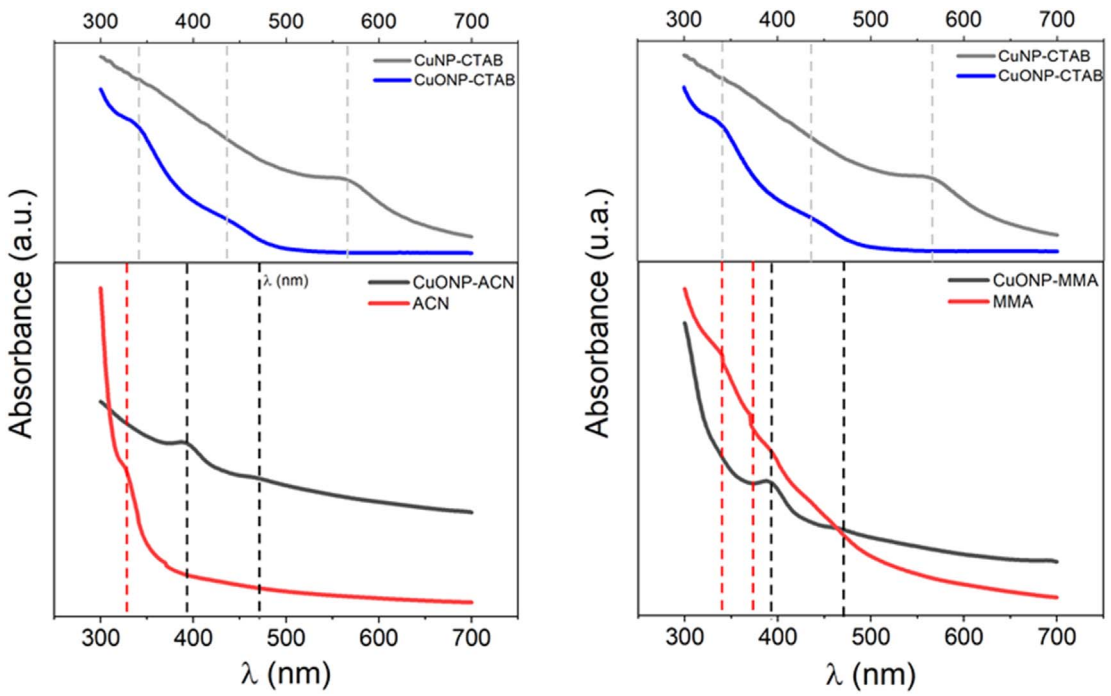


**Figure 1.** Spectra of absorbance of nanoparticles synthesized.

**Table 1.** Surface plasmon resonance of nanoparticles synthesized.

| Entry | Sample | $\lambda_1$ (nm) | $\lambda_2$ (nm) |
|---|---|---|---|
| 1 | CuNP-CTAB | 570 | — |
| 2 | CuONP-CTAB | 340 | 435 |
| 3 | CuONP-ACN | 392 | 470 |
| 4 | CuONP-MMA | 393 | 471 |
| 5 | ACN | 327 | |
| 6 | MMA | 338 | 374 |

### 2.2. Synthesis of functionalized copper nanoparticles CuONP-ACN and CuONP-MMA

The CuONP were produced by sonochemical synthesis through the established protocols [31]. First, 7.5 ml of NaOH (4.4 mm) and 7.5 ml of CTAB (16 mm) were added to a glass vial and homogenized in an ultrasonic bath at 30 °C for 5 min. Then, 50 $\mu$l $CuSO_4.5H_2O$ (0.4 M) was added to the vial and homogenized for 5 min. After, a cold and freshly prepared solution of 100 $\mu$l $NaBH_4$ (2 M) was rapidly aggregated. Finally, the reaction was kept in an ultrasonic bath for 15 min, and then the vial was capped and stored at 23 °C. When the colloidal suspension turned yellow, the CuONP were obtained with a concentration of 0.33% wt. The CuONP-ACN and CuONP-MMA were obtained by the displacement of the CTAB stabilizer by the respective polar monomer (ACN or MMA). The displacement of CTAB was carried out 24 h after that CuONP was obtained. A solution of CuONP synthesized (0.33% wt, 5 ml) was homogenized with 256 $\mu$l of polar monomer (ACN and MMA 0.8 M, which is in excess with respect to the CTAB concentration, 100:1 monomer:CTAB) by magnetic stirring at room temperature for 30 min. After this time, the sample was centrifuged at 13000 rpm for 10 min. The supernatant solution was removed and the nanoparticles were washed once with the monomer solution (256 $\mu$l of monomer 0.8 M in 5 ml of Mili-Q water). The nanoparticles obtained were stored in the monomer solution 0.04 M (volume 5 ml).

### 2.3. Characterization

The functionalized copper nanostructures (CuONP-ACN and CuONP-MMA) were characterized by different techniques. Absorption spectra were obtained by UV–vis absorption spectroscopy from a V-630, Jasco. The chemical structures of the nanoparticles were evaluated using a Fourier-transform infrared spectrometer (FT/IR-4100, Jasco). A Zetasizer, Nano ZS90 was employed to obtain the hydrodynamic diameter and Zeta potential.

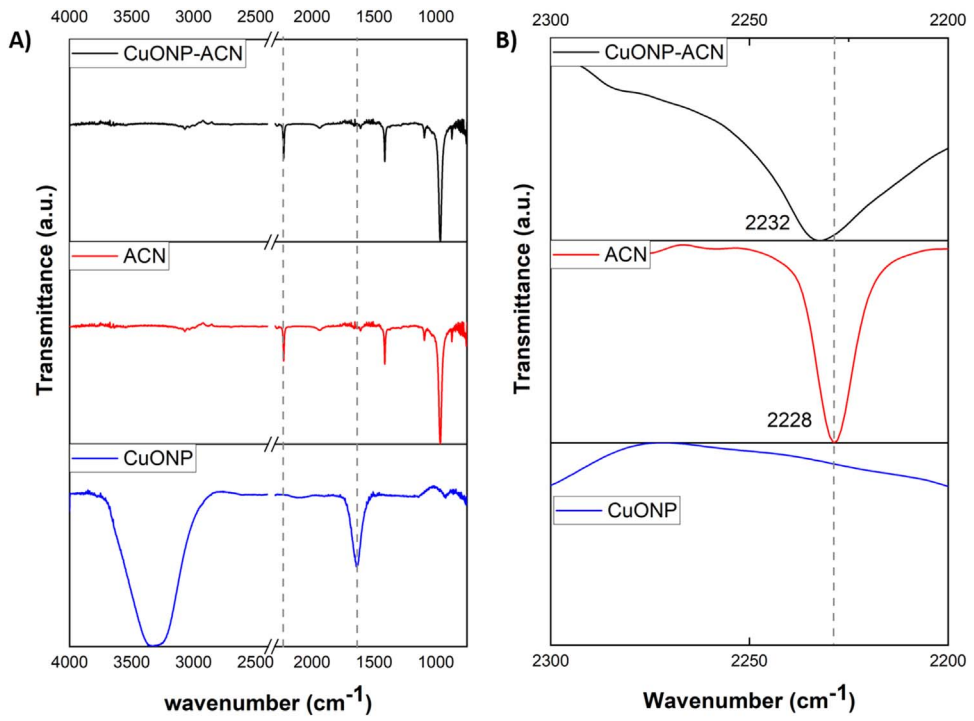


**Figure 2.** (A) FTIR spectra of CuONP-ACN (black line), ACN (red line) and CuONP (blue line). (B) Broadening zone (2000–2200 $cm^{-1}$) for FTIR spectra of CuONP-ACN (black line), ACN (red line) and CuONP (blue line).

The x-ray diffraction was carried out in a Bruker D8 Advance, K$\alpha$1 Cu ($\lambda = 1.5406$ nm) for the determination of the product's crystalline structure. For determination of the size, shape, and phases present in the product, an HR-TEM and selected area electron diffraction (SAED) analysis was carried out in an FEI 2005, model Tecnai ST F120, 80–120 and also in STEM Philips Tecnai 12 (Biotwin).

## 3. Results and discussion

Spectroscopy is a very useful tool for the characterization of MNP, due to the special optical properties that the nanostructured matter presents, with respect to the macroscopic scale. MNP may have a surface plasmon resonance (SPR) with maximum absorption at a specific wavelength which characterizes them; this property is dependent on both the nature of the metal and the size, shape, and interactions between the particles [32].

The UV–vis spectra and the SPR resonance of the CuNP colloidal dispersion and CuONP with the different stabilizers are shown in figure 1 and table 1, respectively. At the top of the figure 1, two absorption spectra are observed. The first corresponds to the synthesized CuNP (gray line) and the second corresponds to the oxidation of these CuNP, producing CuONP (blue line). It should be noted that this oxidation was visualized by a change in color from reddish (CuNP) to yellow (CuONP) and by a shift of the absorption band from 550 to 430 nm [33, 34]. It has been reported that copper oxide has an intense yellow color due to complexation between Cu and O atoms that occurs with an original weak absorption band between 400–500 nm and UV bands of significant intensity corresponding to oxides [35]. The bottom of figure 1 shows the UV–vis spectrum of the CuNP stabilized with ACN (black line). It is possible to see a redshift and a smaller broadening of the absorption bands when the CTAB is displaced by ACN. It is known that the SPR can be tuned by changing the shape, size, composition, and interparticle spacing of NP [36, 37]. In addition, a redshift of the plasmonic peak has been related to the nanoparticle oxidation [38]. Therefore, the presence of conjugated functional groups in the ACN monomer used as stabilizing could have changed the electron density of the new nanoparticle like a nanoparticle oxidation producing the SPR shift. Thus, changing in the SPR suggest the replacement of CTAB by ACN during the ligand exchange reaction. Furthermore, the broadening and the shifting of the band observed between 400 and 500 nm could suggest that a change in the size of the new nanoparticle occurred. The intensity and peak position of the absorption spectrum are specified by the amount and the diameter of NP, respectively. Furthermore, the absorption at longer wavelengths due to scattering of light by large particles [37, 39, 40]. The same behavior was observed in the nanoparticles synthesized by the CTAB displaced by MMA. Moreover, it is known that the polar monomers

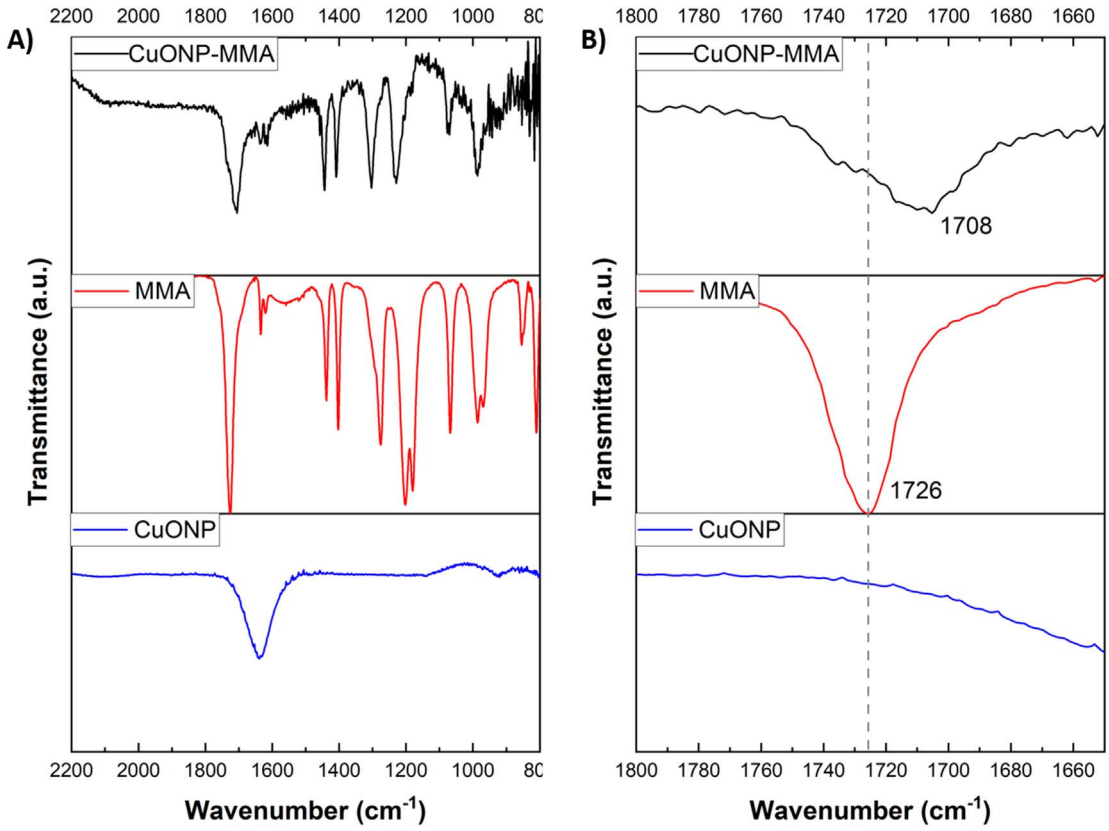


**Figure 3.** (A) FTIR spectra of CuONP- MMA (black line), MMA (red line) and CuONP (blue line). (B) Broadening zone (1800–1600 $cm^{-1}$) for FTIR spectra of CuONP- MMA (black line), MMA (red line) and CuONP (blue line).

present an absorption band in the ultraviolet region around 200 nm to ACN [41] and 240 nm to MMA [42] which confirms that the observed absorption band corresponds to the new conjugated nanoparticles CuONP-ACN and CuONP-MMA.

Furthermore, the FTIR characterization was used to confirm the CTAB displacement by polar monomer in the synthesized nanoparticles. Figure 2 shows a comparison between the FTIR spectra of CuONP synthesized with ACN and the spectra of the precursors used for the synthesis. In the figure 2(A) is possible to observe that the FTIR spectrum of CuONP stabilized with CTAB (blue line) shows two strong signals. The first signal close to 1500 $cm^{-1}$ corresponding to $CH_2$ groups of pure CTAB [43], and this signal does not appear in the FTIR spectra of CuONP-ACN (black line) which suggests the CTAB displacement by ACN. The second signal around to 3500 $cm^{-1}$ may be originated from adsorbed water, and the intensity of this signal was remarkably reduced by ligand exchange from CTAB to ACN. This behavior may be attributed to the differences in the chemical structure of both ligands. The CTAB is a cationic surfactant and the ACN is a polar organic monomer and consequently they interact with the water molecule by different way changing your hydration capacity. In addition, a broadening of FTIR spectra of CuONP-ACN and its synthesis precursors in the zone between 2000 and 2200 $cm^{-1}$ (figure 2(B)) shows that the vibration band corresponding to the main functional group nitrile (CN) presents in the ACN monomer is observed at 2228 $cm^{-1}$ to free monomer (red line), while the spectrum of nanoparticles stabilized by this monomer (CuONP-ACN, black line) shows a red shift of 4 $cm^{-1}$ for this signal. This could indicate that bond length decreases due to the interaction of the nanoparticles with the monomer. It is known that the coordination of CN groups of acrylonitrile with a metal center produces a red displacement of the CN group signal [44]. Moreover, the FTIR spectrum of nanoparticles stabilized with CTAB (CuONP-CTAB), which was employed as a precursor to synthesis, did not show the signal of CN vibrational mode around 2200 $cm^{-1}$. In this context, it can be said that the formation of CuO nanoparticles stabilized with ACN is confirmed.

On the other hand, figure 3(A) shows the spectra of nanoparticles stabilized with MMA (CuONP-MMA). In this case, the ester carbonyl group stretching vibration, C=O peaks are observed at 1726 $cm^{-1}$ for monomer free (red line) and at 1708 $cm^{-1}$ for CuONP-MMA (black line). The shift of the ester carbonyl group stretching vibration to lower wavenumbers could be attributed to the interaction of the carboxylic acid and carboxylate groups of MMA with the metal center of nanoparticles. The interaction of silver nanoparticles with carboxylic acid and carboxylate groups associated with MMA produced the shift of the ester carbonyl group stretching vibration to lower wavenumbers [45]. These results suggest that the obtained nanoparticles (CuONP-ACN and

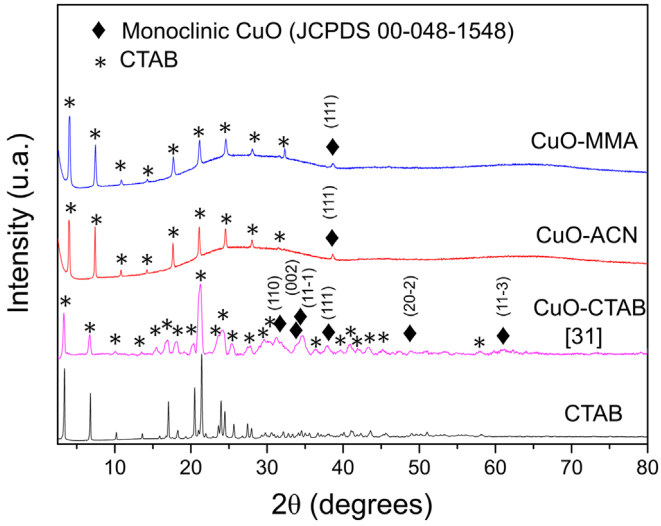


**Figure 4.** XRD patterns of CuONP with different stabilizers.

CuONP-MMA) are stabilized by functional groups present in the respective polar monomer and that this stabilization is achieved by a Pearson acid-base interaction in which the copper metal center in the nanoparticle has an acid character and each monomer ACN and MMA presents a basic character.

The crystal structure was studied by x-ray diffraction (XRD) in a Bruker D8 Advance, K$\alpha$1 Cu ($\lambda = 1.5406$ nm). Figure 4 shows the copper oxide nanoparticle diffractograms with different stabilizing agents (MMA, ACN, and CTAB). The diffractogram represented by the magenta curve [31] corresponding to the CuONP stabilized with CTAB. This diffractogram shows the presence of six crystalline planes indexed in the monoclinic system. The crystalline planes that should present greater intensity in their peaks correspond to planes (1 1 -1) (100% of intensity) and (1 1 1) (99% of intensity) (JCPDS 00-048-1548), which is appreciable in our previous work [33]. The low intensity of the signals with respect to the stabilizer signals is due to the low concentration of the nanoparticles in the stabilizing medium and to the deviation of the diffractogram background, which shows the amorphous structure of the stabilizers (MMA and ACN) and masks the peaks coming from the CuO crystalline phase. Due to this, it is possible only to observe one signal, related to the crystalline plane (1 1 1) of the monoclinic phase of CuO using MMA and ACN as stabilizing agents. The diffractograms corresponding to the nanoparticles stabilized by MMA and ACN do not show the presence of the peak corresponding to the plane (1 1 -1) which should have an intensity comparable to the plane (1 1 1). However, this strong signal located at $2\theta = 35.5^{\circ}$ is masked by the signal of the amorphous stabilizing agents in both cases which is observed in figure 4. In addition, it is possible to observe the presence of sharps peaks in the diffractograms of CuONP stabilized by MMA and ACN which is related to the remaining CTAB in these samples. The presence of these peaks in the diffractograms of CuONP-MMA and CuONP-CAN but not in the respective FTIR spectra is attributed to the sensitivity of each technique.

The diffractograms presented in figure 4 do not allow for a very precise analysis of the presence of CuO (monoclinic) or other crystalline phases such as $Cu_2O$ (cubic). That is why the synthesized nanoparticles were studied by electronic diffraction. The selected area electron diffraction (SAED) patterns of CuO nanoparticles are presented in figure 5. An estimate of interplanar distance allowed both patterns to be indexed in the monoclinic system. The interplanar distance values are very close to those reported for CuO in our previous work using CTAB as a stabilizing agent [31]. Therefore, it can be assured that the product obtained from the synthesis is CuO nanoparticles with a monoclinic structure. In addition, no secondary phases are detected in the SAED patterns with either of the two stabilizing agents.

Besides, the Z potential of the synthesized NP were determined in order to know the surface charge of the new nanoparticles and confirm the displacement of the CTAB stabilizer by the polar monomers. Both, the CuONP-ACN and the CuONP-MMA showed negative Zeta potential (table 2), while the CuONP stabilized with CTAB showed a Zeta potential of $+27.98 \pm 0.9$ mV, herein it indicates an efficient displacement of CTAB by each polar monomer (table 2). Regarding to the hydrodynamic diameter obtained by DLS, it is observed that the CuONP-MMA are larger than the CuONP-ACN (table 2). This could be due to the structural characteristics of polar monomers used to stabilize the nanoparticles. First, the MMA chain size is larger than ACN chain size, and the MMA containing methyl groups with free rotation that require special arrangement and it could increase the dynamic diameter around of nanoparticle. Second, the MMA containing two potential sites to stabilize the

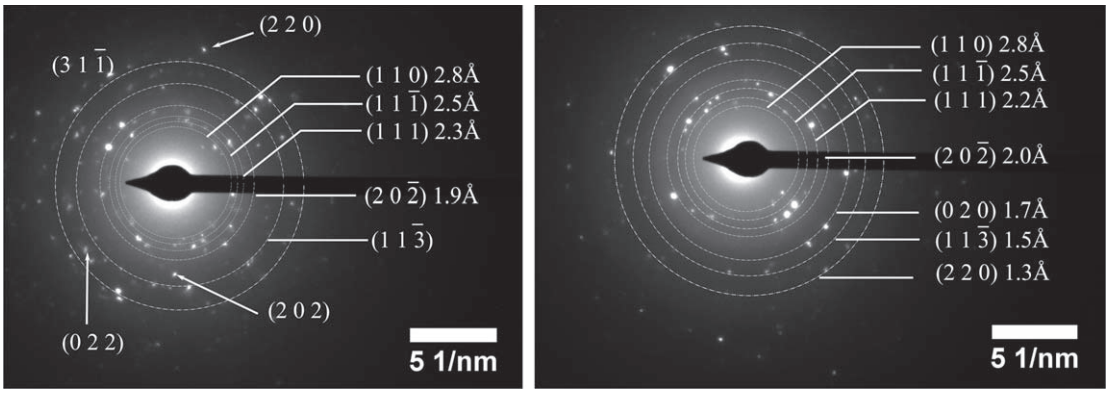


**Figure 5.** Electron diffraction and SAED pattern of CuONP stabilized with (a) ACN and (b) in MMA.

**Table 2.** Hydrodynamic diameter and Zeta potential of NPCuO-CAN and NPCuO-MMA.

| Sample | Intensity (nm) | Volumen (nm) | Number (nm) | PDI | Z (mV) |
|---|---|---|---|---|---|
| NPCuO-ACN | 123 ± 3 | 92 ± 5 | 71 ± 2 | 0.138 ± 0.008 | −(32.9 ± 5.6) |
| NPCuO-MMA | 218 ± 20 | 199 ± 24 | 127 ± 5 | 0.23 ± 0.04 | −(38.4 ± 0.9) |

nanoparticle, these are the carbonyl group and the oxygen of the ester group, which could allow the growth of larger nanoparticles compared to the ACN, which contains only the nitrile functional group as a potential site stabilizer. Third, the copper oxide nanoparticle used as precursor might activate MMA monomers [46] to produce small oligomer chains and consequently large size nanoparticles. Whilst, the ACN monomer used as a stabilizer to CuONP-ACN requires stronger conditions to promote its oligo/polymerization.

In order to determine the shapes and size of the nanoparticles, the samples were studied by SEM and TEM. Figure 6 shows SEM images for precursor nanoparticles (CuONP, 6A) and nanoparticles stabilized with different polar monomers (CuONP-ACN, 6B, CuONP-MMA, 6C). The images show that the nanoparticles used as precursors have a spherical morphology and that this morphology is preserved when the CTAB is displaced by both monomers (figures 6(B), (C)). It has been reported that the shape of copper nanoparticles can be regulated during the synthesis through the variation of the type of surfactant as a stabilizer and the concentration thereof, when CTAB or SDS (sodium sulphate dodecyl) were used as a stabilizer. In this case, the CTAB concentration was above the critical micellar concentration (CMC), which corresponds to the formation of spherical nanoparticles, and subsequently the replacement of the CTAB by polar monomers preserved the spherical morphology.

On the other hand, the figure 7 shows the TEM imagens of CuO nanoparticles stabilized with different polar monomers and their size distribution histogram. From these results was possible to observe that both nanoparticles show two size distributions with size of 32.8 ± 0.3 nm and 4.5 ± 0.2 nm for CuONP-ACN and size of 30 ± 1 nm and 1.24 ± 0.04 nm for CuONP-MMA. The aforementioned behavior could be attributed the destabilization of the NP produced when they were exposed to electron beam irradiation. The capping agents used for the stabilization of both nanoparticles are polar organic monomers, and it is known that this type of capping agents can cause difficulty in resolving atomic structures of coalesced NP [47], or can be easily susceptible to damage under electron beam irradiation, which behave like bare NP [48, 49]. Consequently, two populations with different size distribution for each nanoparticle are produced, and the average size of the nanoparticles determined by DLS turned out to be larger than the size of the nanoparticles determined by TEM.

## 4. Conclusions

The functionalization of copper oxide nanoparticles by two polar monomers (that are of commercial interest), such as ACN and MMA was efficiently achieved using a ligand exchange reaction from CuONP-CTAB. The replacement of the CTAB stabilizer by ACN or MMA polar monomer produced a dramatic change in the surface charge of nanoparticles generating CuONP-ACN and CuONP-MMA with a Zeta potential of −32.9 ± 5.6 mV and −38.4 ± 0.9 mV, respectively. CuONP-ACN was found to have a smaller size than CuONP-MMA, which

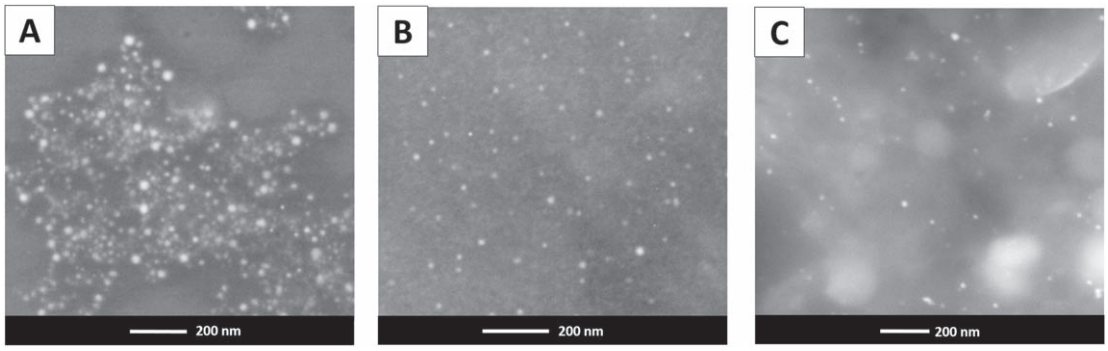


**Figure 6.** SEM images. (A) CuONP (CTAB), (B) CuONP-ACN, (C) CuONP-MMA.

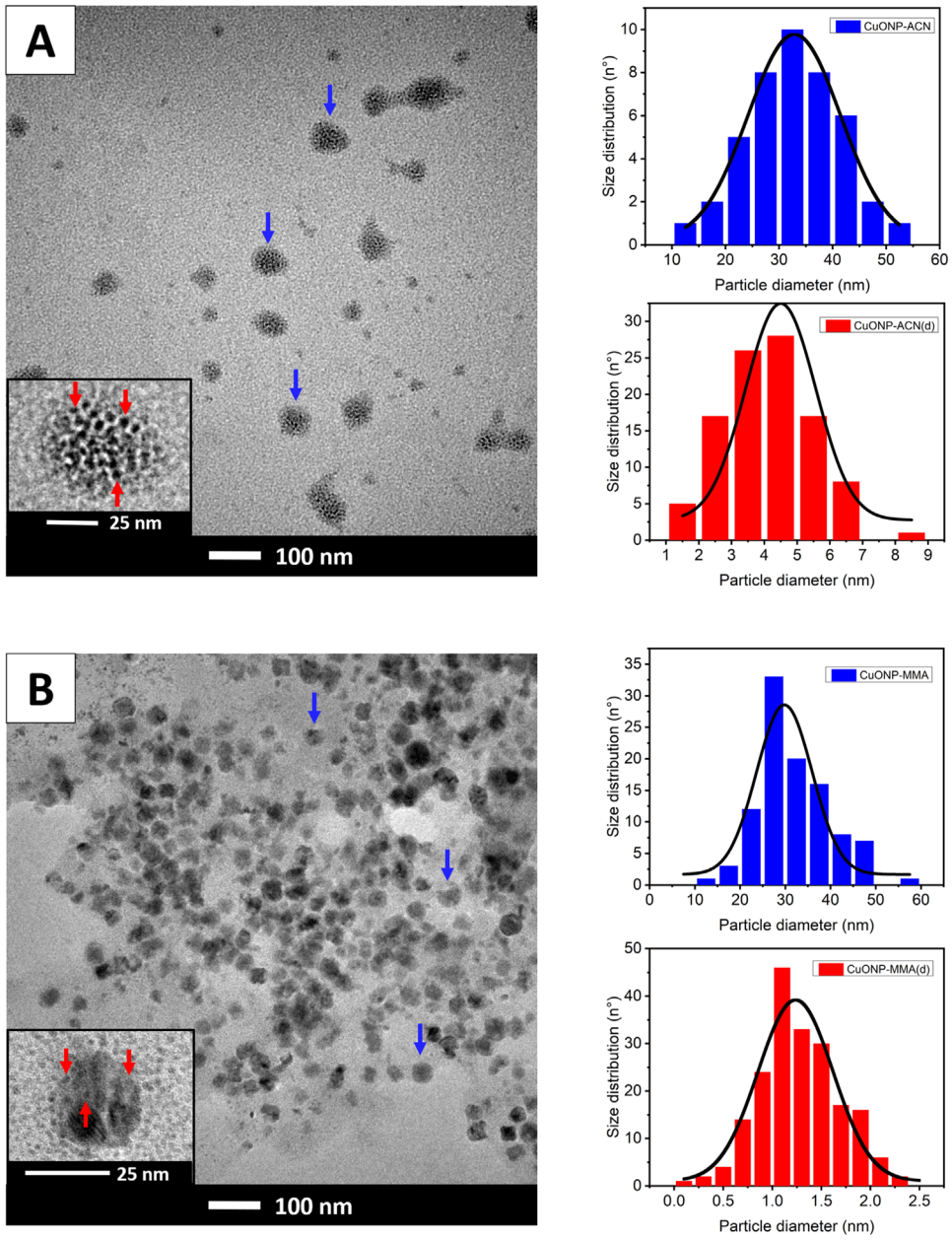


**Figure 7.** TEM micrographs of (A) CuONP-ACN (B) CuONP-MMA with their respective particle size distribution histograms (blue color). The insert shows a higher magnification of a nanoparticles destabilized by electron beam irradiation with their respective particle size distribution histograms (red color).

might be attributed to MMA containing: (a) methyl groups with free rotation that require a special arrangement, (b) two potential sites to stabilize the nanoparticle, and (c) the possible formation of an MMA oligomer. The aforementioned features might increase the dynamic diameter of the CuONP-MMA.

These new functionalized NP can potentially improve interfacial interactions between their surfaces and the polymer matrix. Hence, future studies should attempt to incorporate these new functionalized nanoparticles in a polar polymer matrix and investigate the properties of the modified material.

## Acknowledgments

The authors thank the Associative Research Program of the National Commission of Science and Technology (CONICYT, PIA Project ACM170003). Iván Martínez thanks CONICYT, FONDECYT/Postdoctoral 3160480. Proyecto Fondequip EQM150101 for a collaboration in SEM imaging. Bárbara Rodríguez thanks CONICYT, FONDECYT/Postdoctoral 3180093.

## Data availability statement

All data that support the findings of this study are included within the article (and any supplementary files).

## Declarations

Not applicable

## Funding

This study was funded by CONICYT, PIA Project ACM170003 and CONICYT, FONDECYT/Postdoctoral 3160480.

## Conflict of interest

The authors declare that they have not conflict of interest.

## Author contributions

B R, experimental work related to synthesis material and writing of results, S R, Experimental work related to synthesis and characterization of material, P G, postgraduate student experimental work related to synthesis material, N S, conceptualization and editing of the manuscript, I D-A selected area electron diffraction (SAED) patterns analysis, A G editing of the manuscript and funding acquisition and I M, idea conceptualization, editing of the manuscript and funding acquisition.

## ORCID iDs

Iván Martínez https://orcid.org/0000-0002-4434-5970

## References

[1] Mandal D, Bolander M E, Mukhopadhyay D, Sarkar G and Mukherjee P 2006 The use of microorganisms for the formation of metal nanoparticles and their application *Appl. Microbiol. Biotechnol.* **69** 485–92
[2] Jayaseelan C, Ramkumar R, Rahuman A A and Perumal P 2013 Green synthesis of gold nanoparticles using seed aqueous extract of Abelmoschus esculentus and its anti-fungal activity *Ind. Crops Prod.* **45** 423–9
[3] Basavegowda N, Idhayadhulla A and Lee Y R 2014 Preparation of Au and Ag nanoparti-cles using Artemisia annua and their *in vitro* antibacterial and tyrosinase inhibitory activities *Mater. Sci. Eng. C* **43** 58–64
[4] Yusuf M 2019 Silver nanoparticles: synthesis and applications *Handbook of Ecomaterials.* ed L Martínez, O Kharissova and B Kharisov (Cham: Springer) (https://doi.org/10.1007/978-3-319-68255-6_16)
[5] Kang X, Mai Z, Zou X, Cai P and Mo J 2007 A sensitive nonenzymatic glucose sensor in alkaline media with a copper nanocluster/multiwall carbon nanotube-modified glassy carbon electrode *Anal. Biochem.* **363** 143–50
[6] Yang G J, Xu J J, Wang K and Chen H Y 2006 Electrocatalytic oxidation of dopamine and ascorbic acid on carbon paste electrode modified with nanosized cobalt phthalocyanine particles: simultaneous determination in the presence of CTAB *Electroanalysis* **18** 282–90

[7] Lakshmi Kantam M, Swarna Jaya V, Jaya Lakshmi M, Reddy B R, Choudary B M and Bhargava S K 2007 Alumina supported copper nanoparticles for aziridination and cyclopropanation reactions *Catal. Commun.* **8** 1963–8
[8] Rodriguez J A, Liu P, Hrbek J, Evans J and Pérez M 2007 Water gas shift reaction on Cu and Au nanoparticles supported on $CeO_2$(111) and ZnO(0001): intrinsic activity and importance of support interactions *Angewandte Chemie—International Edition* **46** 1329–32
[9] Cioffi N *et al* 2005 Copper nanoparticle/polymer composites with antifungal and bacteriostatic properties *Chem. Mater.* **17** 5255–62
[10] Din M I and Rehan R 2017 Synthesis, characterization, and applications of copper nanoparticles *Anal. Lett.* **50** 50–62
[11] Khodashenas B and Ghorbani H R 2014 Synthesis of copper nanoparticles: an overview of the various methods *Korean J. Chem. Eng.* **31** 7 New York LLC: Springer 1105–1109
[12] Sharma V K, Yngard R A and Lin Y 2009 Silver nanoparticles: green synthesis and their antimicrobial activities *Adv. Colloid Interface Sci.* **145** 83–96
[13] Liu Q M, Zhou D B, Yamamoto Y, Ichino R and Okido M 2012 Preparation of Cu nanoparticles with $NaBH_4$ by aqueous reduction method *Transactions of Nonferrous Metals Society of China (English Edition)* **22** 117–23
[14] Xiong J, Wang Y, Xue Q and Wu X 2011 Synthesis of highly stable dispersions of nanosized copper particles using l-ascorbic acid *Green Chem.* **13** 900–4
[15] Wu S H and Chen D H 2004 Synthesis of high-concentration Cu nanoparticles in aqueous CTAB solutions *J. Colloid Interface Sci.* **273** 165–9
[16] Ranjbar-Karimi R, Bazmandegan-Shamili A, Aslani A and Kavian K 2010 Sonochemical synthesis, characterization and thermal and optical ai CuO nanoparticles *Physica B* **405** 3096–100
[17] Zhang J, Wang J, Fu Y, Zhang B and Xie Z 2015 Sonochemistry-synthesized CuO nanoparticles as an anode interfacial material for efficient and stable polymer solar cells *RSC Adv.* **5** 28786–93
[18] Korala L and Prieto A L 2017 Chemical functionalization of colloidal inorganic nanocrystals (NCs) via ligand exchange *Reference Module in Chemistry, Molecular Sciences and Chemical Engineering* (*Enciclopedy of Interfacial Chemistry: Surface Science and Electrochemistry*) (Amsterdam: Elsevier) 1–10
[19] Gao P, Xiao G, Wang L, Chen Y, Wang Y and Zhang G 2011 Ultrasonochemical-assisted synthesis of CuO nanorods with high hydrogen storage ability *Journal of Nanomaterials* **2011** 1–6
[20] Karunakaran C, Manikandan G and Gomathisankar P 2013 Microwave, sonochemical and combustion synthesized CuO nanostructures and their electrical and bactericidal properties *J. Alloys Compd.* **580** 570–7
[21] Smith A M *et al* 2015 Quantitative analysis of thiolated ligand exchange on gold nanoparticles monitored by 1H NMR spectroscopy *Anal. Chem.* **87** 2771–8
[22] Locardi F *et al* 2018 Thermogravimetry and evolved gas analysis for the investigation of ligand-exchange reaction in thiol-functionalized gold nanoparticles *J. Anal. Appl. Pyrolysis* **132** 11–8
[23] Kluenker M, Mondeshki M, Nawaz Tahir M and Tremel W 2018 Monitoring thiol-ligand exchange on au nanoparticle surfaces *Langmuir* **34** 1700–10
[24] Yi M, Kim W S, Park B J, Lee B, Bhang S H and Yu T 2016 A facile surface modification of polyethylenimine-stabilized gold nanoparticles and their enhanced cytotoxicity *J. Nanosci. Nanotechnol.* **16** 7043–8
[25] Mao X, Kwon J, Koh E K, Hwang D Y and Lee J 2015 Ligand exchange procedure for bimetallic magnetic iron-nickel nanocrystals toward biocompatible activities *ACS Appl. Mater. Interfaces* **7** 15522–30
[26] Palma S I C J, Marciello M, Carvalho A, Veintemillas-Verdaguer S, Morales M. del P. and Roque A C A 2015 Effects of phase transfer ligands on monodisperse iron oxide magnetic nanoparticles *J. Colloid Interface Sci.* **437** 147–55
[27] Hatakeyama M *et al* 2011 A two-step ligand exchange reaction generates highly water-dispersed magnetic nanoparticles for biomedical applications *J. Mater. Chem.* **21** 5959–66
[28] Davis K, Qi B, Witmer M, Kitchens C L, Powell B A and Mefford O T 2014 Quantitative measurement of ligand exchange on iron oxides via radiolabeled oleic acid *Langmuir* **30** 10918–25
[29] Wang X, Tilley R D and Watkins J J 2014 Simple ligand exchange reactions enabling excellent dispersibility and stability of magnetic nanoparticles in polar organic, aromatic, and protic solvents *Langmuir* **30** 1514–21
[30] Lattuada M and Hatton T A 2007 Functionalization of monodisperse magnetic nanoparticles *Langmuir* **23** 2158–68
[31] Silva N, Ramírez S, Díaz I, Garcia A and Hassan N 2019 Easy, quick, and reproducible sonochemical synthesis of CuO nanoparticles *Materials* **12** 5
[32] Sosa I O, Noguez C and Barrera R G 2003 Optical properties of metal nanoparticles with arbitrary shapes *J. Phys. Chem. B* **107** 6269–75
[33] du Cao V, Tran N Q and Nguyen T P P 2015 Synergistic effect of citrate dispersant and capping polymers on controlling size growth of ultrafine copper nanoparticles *J. Exp. Nanosci.* **10** 576–87
[34] Wang Y and Asefa T 2010 Poly(allylamine)-stabilized colloidal copper nanoparticles: synthesis, morphology, and their surface-enhanced raman scattering properties *Langmuir* **26** 7469–74
[35] Sierra-Ávila R *et al* 2014 Synthesis of copper nanoparticles coated with nitrogen ligands *J. Nanomater.* **2014** 361791
[36] Jain P K, Huang X, El-Sayed I H and El-Sayed M A 2008 Noble metals on the nanoscale: optical and photothermal properties and some applications in imaging, sensing, biology, and medicine *Acc. Chem. Res.* **41** 1578
[37] Eustis S and El-Sayed M A 2006 Why gold nanoparticles are more precious than pretty gold: noble metal surface plasmon resonance and its enhancement of the radiative and nonradiative properties of nanocrystals of different shapes *Chem. Soc. Rev.* **35** 209
[38] Yaremchuk I, Meškinis Š, Bulavinets T, Vasiliauskas A, Andrulevičius M, Fitio V, Bobitskia Y and Tamulevičius S 2019 Effect of oxidation of copper nanoparticles on absorption spectra of DLC:Cu nanocomposites *Diamond & Related Materials* **99** 107538
[39] Xu B, Song R G, Tang P H, Wang J, Chai G Z, Zhang Y Z and Ye Z Z 2008 Preparation of Ag nanoparticles colloid by pulsed laser ablation in distilled water *Key Eng. Mater.* **373–374** 346
[40] Moniri S, Ghoranneviss M, Hantehzadeh M R and Asadabad M A 2017 Synthesis and optical characterization of copper nanoparticles prepared by laser ablation *Bull. Mater. Sci.* **40** 37–43
[41] Fikhtengol'ts V S, Zolotareva R V and L'vov Y A 1966 *Ultraviolet Spectra of Elastomers and Rubber Chemicals.* 1 (United States of America: Springer) 170
[42] Barth J A, Brunn J, Peters F and Dethlopf M 1976 *J. Prakt. Chem.* **318** 745
[43] Amin S *et al* 2016 *Journal of Environmental Chem. Eng.* **4** 3825–34
[44] Hume A S and Fry F 1968 *Department of Pharmacology and Toxicology* (Oxford: Pergamon) 466
[45] Darman Singho N, Akmal Che Lah N, Rafie Johan M and Ahmad R 2012 FTIR studies on Silver-Poly(Methylmethacrylate) nanocomposites via in-situ polymerization technique nano-bio-sensors view project carbon nanotubes view project FTIR Studies on Silver-Poly(Methylmethacrylate) nanocomposites via in-situ polymerization technique *Int. J. Electrochem. Sci.* **7** 5596–603

[46] Moustafa A B, Radwan F M and Emam A 1990 Heterogeneous polymerization of methyl methacrylate in absence and presence of surface modified cuprous oxide *Journal of Applied Polymer Science* **41** 2021–30
[47] Tan S F, Bosman M and Nijhuis C A 2017 Molecular coatings for stabilizing silver and gold nanocubes under electron beam irradiation *Langmuir* **33** 1189–96
[48] Azcárate J C, Fonticelli M H and Zelaya E 2017 Radiation damage mechanisms of monolayer-protected nanoparticles via TEM analysis *J. Phys. Chem. C* **121** 26108–16
[49] Yu Y *et al* 2016 Atomic structure of ultrathin gold nanowires *Nano Lett.* **16** 3078–84